The CIRCE simulations : Regional Climate Change Projections with Realistic Representation of the Mediterranean Sea

S. Gualdi, S. Somot, L. Li, V. Artale, M. Adani, A. Bellucci, A. Braun, S. Calmanti, A. Carillo, A. Dell'Aquila, et al.

HAL Id: hal-01103544
https://hal.archives-ouvertes.fr/hal-01103544

Submitted on 19 Jan 2015

THE CIRCE SIMULATIONS
Regional Climate Change Projections with Realistic Representation of the Mediterranean Sea

BY S. GUALDI, S. SOMOT, L. LI, V. ARTALE, M. ADANI, A. BELLUCCI, A. BRAUN, S. CALMANTI, A. CARILLO, A. DELL'AQUILA, M. DÉQUÉ, C. DUBOIS, A. ELIZALDE, A. HARZALLAH, D. JACOB, B. L'HÉVÉDER, W. MAY, P. ODDO, P. RUTI, A. SANNA, G. SANNINO, E. SCOCCIMARRO, F. SEVAULT, AND A. NAVARRA

A multimodel system for the Mediterranean region improves simulation of physical processes involved in the complex, intricate interaction of land, air, and sea.

THE PROBLEM OF THE MEDITERRA-NEAN REGION CLIMATE SIMULA-TIONS. The climate of the Mediterranean region, defined here as the area including the Mediterranean Sea and the surrounding areas, is determined by the interaction between midlatitude and subtropical circulation regimes with the complex morphology (mountain chains and land–sea contrasts) that characterizes this part of Earth. The region has been identified as one of the main climate change hotspots: that is, one of the most responsive areas to climate change (Giorgi 2006). The area is populated by over 500 million people, distributed in about 30 countries in Africa, Asia, and Europe.

Therefore, understanding climate variability here has also important social implications.

In the recent past, a number of scientific initiatives and projects have been undertaken to assess the possible changes that anthropogenic global warming might induce in the climate of the European continent and of the Mediterranean region. Specifically, scenario simulations aimed at quantifying the possible future climate change in the European and Mediterranean region have been designed and performed in the framework of European Union (EU) projects such as the Prediction of Regional Scenarios and Uncertainties for Defining European Climate Change Risks and Effects (PRUDENCE;

Christensen et al. 2007) and Ensemble-Based Predictions of Climate Changes and Their Impacts (ENSEMBLES; Christensen et al. 2009). At the same time, coordinated studies have been performed to investigate and to assess the climate change signal in the Mediterranean region projected by both regional and global models (Giorgi and Lionello 2008). Marcos and Tsimplis (2008), for example, used phase 3 of the Coupled Model Intercomparison Project (CMIP3) data (Meehl et al. 2007) to assess the uncertainty range of the response of the Mediterranean Sea temperature, salinity, and sea level change during the twenty-first century. According to their findings, the CMIP3 general circulation models (GCMs) reveal many difficulties in simulating a realistic Mediterranean Sea in present climate because of their low spatial resolution. Therefore, the climate change signal produced by these models in the Mediterranean region should also be considered with some caution. Using the same dataset, Mariotti et al. (2008) quantified the change in the regional water budget (WB) components. A similar analysis has been done by Sanchez-Gomez et al. (2009), using the outputs of the ENSEMBLES atmosphere-only regional climate models (RCMs), with 25-km resolution over the Mediterranean Sea, for the A1B scenario. Their results show that both global and regional models produce climate scenarios characterized by a significant drying of the Mediterranean region, mainly after year 2050 of the emission scenarios.

Concerning the impact of the climate change on the Mediterranean Sea, so far very few studies have been specifically devoted to this basin. Furthermore, all of these studies were conducted with just one climate model, leaving largely unresolved the fundamental issue of the uncertainty associated with the choice of the model. Pioneering work was done by Thorpe and Bigg (2000), who simulated a transient $2 \times CO_2$ scenario with a 1/4°-resolution ocean model forced by the air–sea fluxes of a low-resolution Intergovernmental Panel on Climate Change (IPCC) model ($2.5° \times 3.5°$). Later, Somot et al. (2006) performed a similar study using a higher-resolution ocean model (1/8°) forced by fluxes coming from a dynamical downscaling (50 km) of an IPCC A2 run. Both studies show an increase of the sea surface temperature (SST) and sea surface salinity (SSS), leading to a strong weakening of the Mediterranean thermohaline circulation (MTHC) and a change in the characteristics of the Mediterranean waters outflowing at the Gibraltar Strait. The latter study took into account the climate change impact coming from all the various forcings of the Mediterranean

Sea (air–sea fluxes, Atlantic characteristics, river runoff, and Black Sea impact), concluding that all of them could be important contributors to the possible evolution of the sea characteristics.

Most of the above-mentioned works are based either on global low-resolution atmosphere–ocean coupled general circulation models (AOGCMs) or stand-alone (atmosphere only or ocean only) high-resolution regional models. Each of two approaches presents advantages and weaknesses. An important shortcoming common to the global coupled and regional atmosphere-only models is their limited capability to include into the climate change projections for this region a realistic representation of the processes associated with the presence of the Mediterranean Sea. The global AOGCMs used so far have horizontal resolutions generally not sufficient to represent the complexity of the geomorphology of the region. Figures 1a,b show the Mediterranean Sea and the surrounding mountain chains (Atlas, Alps, and Caucasus Mountains) as they are represented in a global model with a horizontal resolution of about 300 km in the atmosphere and about 100 km in the ocean. This is the order of resolution employed, for example, in several models used to perform the CMIP3 simulations (Meehl et al. 2007). It appears evident that a number of important features, such as the complex topography, the islands, the straits, and the coastlines of the Mediterranean Sea itself, are only barely resolved. Therefore, these models reproduce the small-scale physical processes that characterize the climate behavior of the region very poorly.

In contrast, the atmosphere-only regional models used so far to downscale the global simulations, such as those employed in the PRUDENCE or ENSEMBLES EU projects, are usually implemented with horizontal resolutions ranging from 50 to 20 km, which according to Gibelin and Déqué (2003) and Gao et al. (2006) should be sufficient to simulate a realistic circulation over the Mediterranean Sea and the European continent. These models, however, are forced with prescribed lower boundary conditions (SSTs), and thus they do not take into account any air–sea feedbacks. The lack of these feedbacks reduces the consistency between SST, air–sea fluxes, and the vertical structure of the atmosphere (air–sea coupling), diminishing the confidence in the modeling results over the Euro–Mediterranean area (Somot et al. 2008). Furthermore, the Mediterranean SSTs used to force the models over the basin are produced with low-resolution AOGCMs, which are inadequate to reproduce the small-scale features that distinguish the behavior of this sea (e.g., Marcos and

Tsimplis 2008). Similar arguments hold for regional ocean-only model simulations, where air–sea feedbacks are not fully considered.

The deficiencies in including a realistic modeling of the Mediterranean Sea in the climate system might have considerable consequences on the quality and reliability of the climate change projections that state-of-the-art models (both global and regional) provide for the Mediterranean area and the European continent. A first attempt to remedy these deficiencies has been made by Somot et al. (2008), who developed an atmosphere–ocean regional climate model (AORCM), coupling a variable-resolution version of a global atmospheric model with a high-resolution oceanic model of the Mediterranean Sea [for additional details, see Somot et al. (2008)]. According to their results, the coupled model appears to be in good agreement with the observations over the Mediterranean region for the reference period 1961–90. Moreover, it appears to perform as well as or even better than most of the PRUDENCE state-of-the-art uncoupled regional models forced with observed SSTs in the Mediterranean basin. Importantly, Somot et al. (2008) found also substantial differences between

the regional coupled and uncoupled climate change projections, which can be ascribed to the inclusion of the Mediterranean Sea model.

In the framework of the Climate Change and Impact Research: The Mediterranean Environment (CIRCE) EU project, a set of coupled models has been developed with the aim of producing climate change projections for the Mediterranean region. Following Somot et al. (2008), all of the models include a high-resolution numerical model of the Mediterranean Sea, and thus they can simulate the small-scale features of the basin. They have been integrated to produce multimodel ensemble simulations of the present climate and future change projections. The multimodel ensemble approach adopted in CIRCE is one of the techniques most frequently used to assess the uncertainties that can arise from different types of model errors (Déqué et al. 2007). This approach provides an estimate of the uncertainty due to structural variations among a range of models by combining them, with the main assumption of a quasi-independent development of the considered models and excluding any systematic analysis of individual sources of errors. In general, the multimodel ensemble
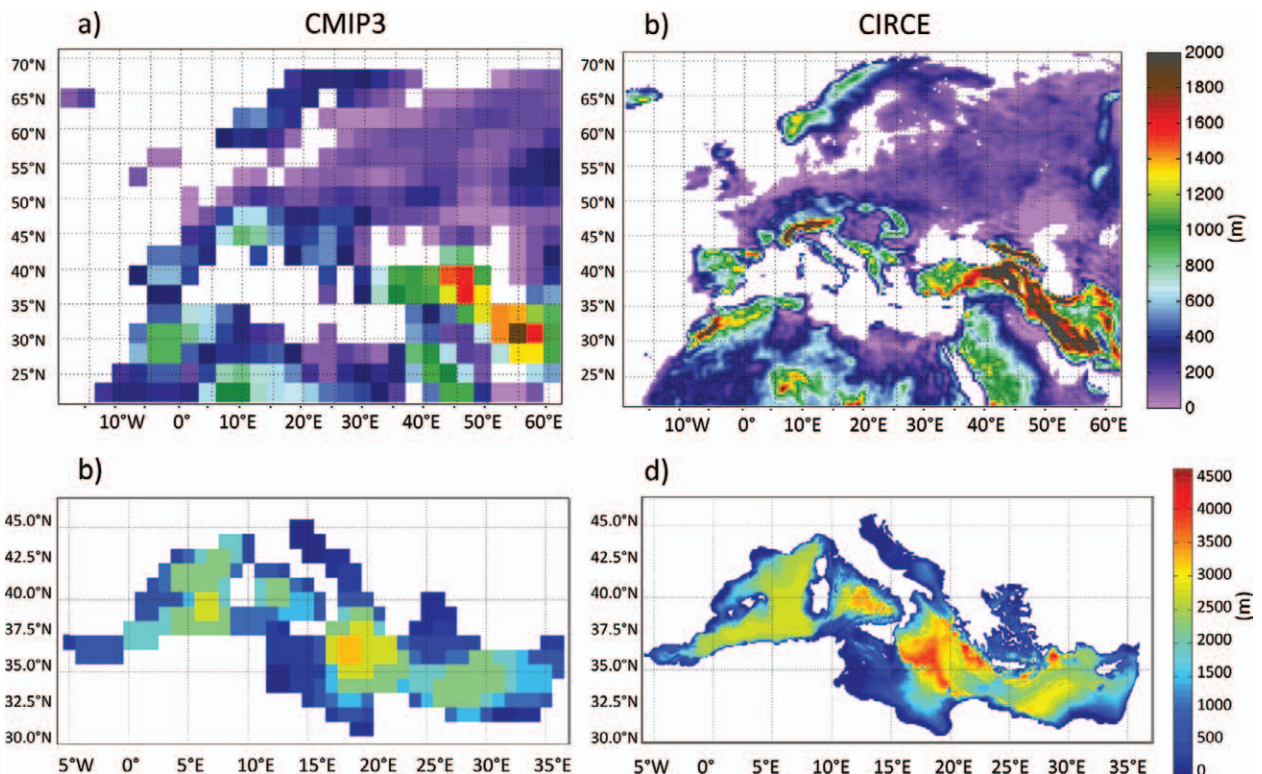
FIG. 1. Orography of the Euro–Mediterranean region and bathymetry of the Mediterranean Sea as represented (a),(b) in a state-of-the-art global coupled ocean–atmosphere model with a horizontal resolution of about 300 km in the atmosphere and 1° in the ocean and (c),(d) in the CIRCE models, where in most of the models the resolution is higher than 50 km in the atmosphere and 1/8° in the ocean.

experiments are not specifically designed to provide formal error estimates. They are in essence "ensembles of opportunity," and the ensemble spread can be seen as a tool to characterize the model uncertainty. The CIRCE experiments thus will allow the quantification of the Mediterranean Sea response to climate change, providing also an estimate of the uncertainty associated with the choice of models, though the relatively small size of the multimodel ensemble (five members) will not allow a comprehensive and statistically robust uncertainty assessment.

In the following, we will discuss the basic characteristics of the CIRCE models, their ability to simulate the major features of the observed climate in the Mediterranean region, and how these features might be possibly affected by global warming in the next few decades.

THE CIRCE MODELS. The major novelty featured by the CIRCE models compared with the climate models commonly used to produce scenario simulations is the inclusion of a realistic representation of the Mediterranean Sea into the climate system. To achieve the aim, the CIRCE models include high-resolution atmospheric components fully coupled with high-resolution models of the Mediterranean Sea able to resolve those small-scale features that characterize the physiography of the basin, as is shown in Figs. 1c,d.

Figure 2 provides a schematic representation of the implementation of the CIRCE models. All of the models have a relatively high-resolution atmospheric component over the Mediterranean region (ranging from 80 to 25 km) that can be either stretched/global or limited area over this region. These atmospheric components are coupled with a high-resolution model of the Mediterranean Sea, exchanging local air–sea fluxes. When the atmospheric model is global (Fig. 2, left), the rest of the global ocean is represented by a global low-resolution ocean model coupled with the Mediterranean Sea in the vicinity of the Strait of Gibraltar. When the atmospheric component is regional (Fig. 2, right), the lateral boundary conditions for both the limited-area atmosphere and the Mediterranean Sea models are provided by global simulations.

Table 1 summarizes the main characteristics of the CIRCE models along with references where more detailed descriptions of the models' features and in-depth discussions of the technical aspects are made. Here, for the sake of brevity, we provide only a general overview of the modeling strategy, in order to illustrate the basic characteristics of the CIRCE approach. In three cases [Centro Euro-Mediterraneo per i Cambiamenti Climatici (CMCC), Centre National de Recherches Météorologiques (CNRM), and Laboratoire de Météorologie Dynamique (LMD)], the Mediterranean Sea component is coupled with a global atmosphere and, in a region
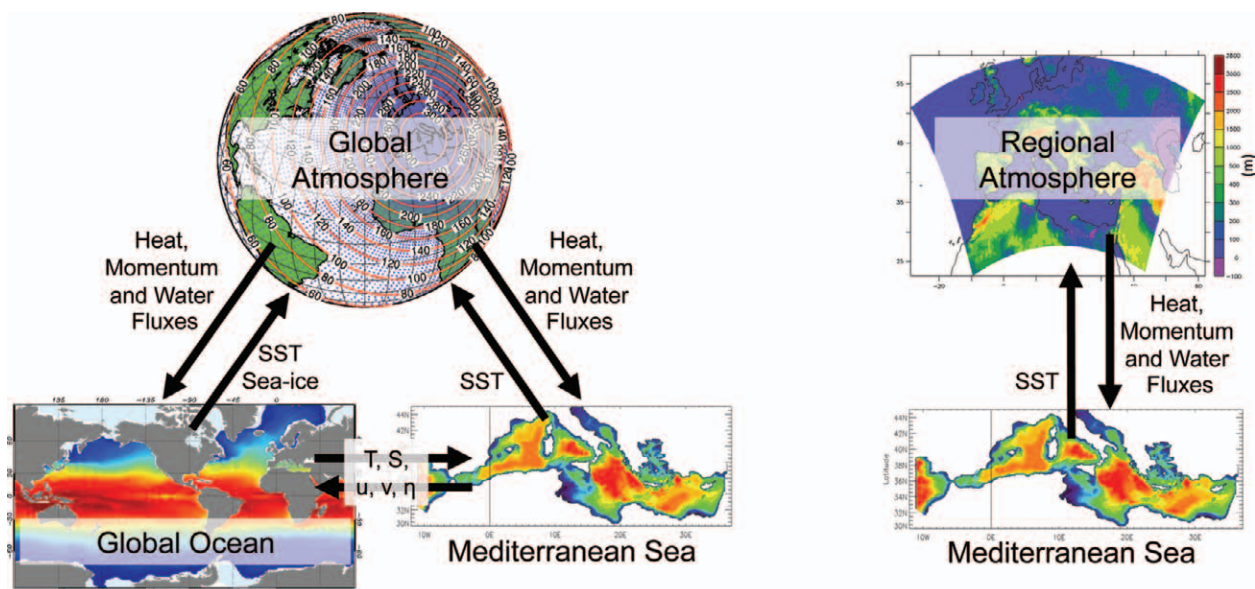
Fɪɢ. 2. Scheme of the basic characteristics of the CIRCE models. (left) Setup of the models with a high-resolution Mediterranean Sea component coupled with a global ocean and a global atmosphere [Istituto Nazionale di Geofisica e Vulcanologia (INGV), L'Institut Pierre-Simon Laplace (IPSL), and Météo-France models]. (right) Setup of the models where the high-resolution Mediterranean Sea component is coupled with a high-resolution limited-area atmospheric model (ENEA and MPI models).

near Gibraltar, with a global ocean. In these models, every atmosphere–ocean coupling time step (~3 h for CMCC and daily for CNRM and LMD), heat (radiative and turbulent fluxes), mass (evaporation, precipitation, and runoff), and momentum fluxes are provided to the ocean models (both global and Mediterranean) by the atmospheric model. At the same time, the atmosphere receives the global SST and the sea ice distribution values from the global ocean and the SST in the Mediterranean Sea from the Mediterranean model. The communications between the oceanic and atmospheric components are carried out with the Ocean Atmosphere Sea Ice Soil [OASIS version 3 (OASIS3)] coupler (Valcke 2006).

The global and Mediterranean ocean components, on the other hand, exchange the coupling fields in a so-called Atlantic box (a relatively large area located to the west of Gibraltar) via oceanic open boundaries, where the exchanged quantities (profiles of temperature, salinity, zonal and meridional velocity, and sea surface elevation) are suitably interpolated. The coupling occurs every 8 h in the CMCC model and on daily basis in the CNRM and LMD models. The Atlantic characteristics in these modes evolved interactively

TABLE 1. Summary of the basic features of the CIRCE models and their implementation. References indicate where a more detailed description of the models, their features, and performances are described and discussed. LMDZ = LMD Model with Zoom Capability. ARPEGE = Action de Recherche Petite Echelle Grande Echelle. RegCM3 = Regional Climate Model version 3; REMO = Regional Model; OPA8.2 = Océan Parallélisé 8.2; ORCA2 = 2° version of the Arakawa grid implemented in the OPA model; NEMO = Nucleus for European Modelling of the Ocean; NEMO-MFS = Mediterranean ocean Forecasting System version of the NEMO model; NEMO-MED8 = Mediterranean version of NEMO at 1/8° resolution; MITgcm = Massachusetts Institute of Technology General Circulation Model; MPI-HH = Max-Planck Institut fuer Meteorologie in Hamburg; TRIP = Total Runoff Integrating Pathways; IRIS = Implementation of River Information Services in Europe.

Model	Atmosphere component	Global ocean component	Mediterranean Sea component	Gibraltar and lateral boundary conditions	Rivers and Black Sea
CMCC (INGV) (Scoccimarro et al. 2011)	**ECHAM5** 80 km, L31	**OPA8.2-ORCA2** grid ~ 2° × 2° (0.5° equator), L31	**NEMO-MFS** 1/16° (~7 km), L71 (Oddo et al. 2009)	Fluxes exchanged between global ocean and Mediterranean Sea. Mediterranean outflow distributed over the upper 300 m in the global ocean grid point near Gibraltar.	TRIP river scheme (Nile runoff corrected to the observations after 1968). Black Sea input from the *E-P-R* flux (Oki and Sud 1998).
LMD (IPSL) (Hourdin et al. 2006; Zou et al. 2010)	**LMDZ global + LMDZ regional** 300 km, L19 + 30 km, L19	**OPA9-ORCA2** ~ 2° × 2° (0.5° equator), L31	**NEMO-MED8** 1/8° (9–12 km), L43 (Beuvier et al. 2010)	Tracer profile and fluxes exchanged using cross-land advection parameterization and buffer zone.	Climatological river discharge (Ludwig et al. 2009).
CNRM (Météo-France/CNRM) (Somot et al. 2008)	**ARPEGE-Climate TL159c2.5**, stretched model: 50 km × 50 km over Euro–Mediterranean–North Africa) L31	**OPA9-ORCA2** ~ 2° × 2° (0.5° equator), L31	**NEMO-MED8** 1/8° (9–12 km), L43 (Beuvier et al. 2010)	Tracer profile and fluxes exchanged using cross-land advection parameterization and buffer zone.	Climatological river discharge (Ludwig et al. 2009).
PROTHEUS (ENEA) (Artale et al. 2010)	**RegCM3** 30 km, L19	—	**MITgcm** 1/8° (9–12 km), L42 (Sannino et al. 2009a)	Atlantic buffer zone. Lateral boundaries from ECHAM5/MPI-OM (Giorgetta et al. 2006).	IRIS river scheme. Instantaneous runoff to the river mouth. Black Sea input from *E-P-R* budget bias corrected.
MPI (MPI-HH) (Elizalde 2011)	**REMO** 25 km, L31	—	**MPI-OM** 9 km, L29 (Elizalde et al. 2010)	Atlantic buffer zone. Lateral boundaries from CMCC (Scoccimarro et al 2011).	Interactive hydrological model and Black Sea model (Hagemann and Jacob 2007).

in the global refined models as the Mediterranean Sea component is fully coupled to the global ocean.

The climate simulations produced with these models (CMCC, CNRM, and LMD) thus account for the regional-scale processes that characterize the Mediterranean basin and provide, for the first time, the possibility to accurately assess the role and feedbacks of the Mediterranean Sea in the global climate system.

In the remaining two models [National Agency for New Technologies, Energy and Sustainable Economic Development (ENEA) and Max Planck Institute (MPI)], the Mediterranean Sea is coupled with a high-resolution atmospheric limited-area component. The coupling, done through OASIS3, is similar to the one implemented for the global models: heat, moisture, and momentum fluxes are passed from the limited-area atmosphere to the Mediterranean Sea component, and the latter returns SSTs to the atmospheric model with a coupling frequency of 6 h. In this case, however, the coupled simulations are conducted prescribing lateral boundary conditions for both the atmosphere and the ocean (in the Atlantic box). Specifically, the lateral boundary conditions for the MPI model are obtained from the CMCC model simulation (Scoccimarro et al. 2011), whereas the ENEA model uses data from the ECHAM5/MPI Ocean Model (MPI-OM) CMIP3 simulations (Giorgetta et al. 2006). Therefore, in contrast with the CMCC, CNRM, and LMD models, where the Mediterranean component is fully coupled to the global ones, in these regional coupled models (ENEA and MPI) the Mediterranean Sea does not provide feedbacks to the global climate system. However, the coupling between the high-resolution atmospheric and Mediterranean Sea components is expected to improve the consistency between SSTs, air–sea fluxes, and the vertical structure of the atmosphere (air–sea coupling) with respect to the coarse-resolution global driver (Dell'Aquila et al. 2011) and thus to better simulate ocean–atmosphere feedbacks, thereby providing more confidence in present and future climate changes over the Mediterranean region (Somot et al. 2008).

Rivers are interactively coupled to the atmosphere and ocean models for ENEA, CMCC, and MPI and are thus impacted by the climate change signals. However, in the CNRM and LMD models, river discharges are kept constant at the observed monthly climatological values, because there is no suitable river-routing scheme. In the scenario simulations, the climatological values of river discharge used in these two models thus are not consistent with the possible changes in land precipitation. A discussion of the implications of this choice has been done in Dubois et al. (2012). However, the river discharge is the smaller component of the water budget in the Mediterranean Sea and the error we make using climatological values is smaller than other approximations we make. For example, in reality in many Mediterranean rivers the actual discharge is strongly modulated by human activities, such as water demand for agriculture purposes (e.g., López-Moreno et al. 2008). These land use changes are only marginally considered in the CIRCE models.

The Black Sea contribution to Mediterranean water budget B is treated differently in the different models. In the MPI case, where the Black Sea is explicitly represented, B is the net water transport computed at the Dardanelles Strait. In the CMCC and in the ENEA models, the B contribution is defined as the residual of the evaporation–precipitation–runoff (E-P-R) budget for this basin in the atmospheric model. Then, following Somot et al. (2006), the budget is used as a freshwater input in the Aegean Sea. However, in the ENEA case, the computed values have been rescaled using monthly coefficients derived from a previous run forced by reanalysis in order to match observations (Dell'Aquila et al. 2011). The LMD and CNRM models, in contrast, used monthly climatological values (Beuvier et al. 2010).

The water budget and heat budget (HB) of the Mediterranean Sea are controlled also by the water exchanges with the Atlantic Ocean, through the Strait of Gibraltar. Such exchanges are highly variable, with strong fluctuations ranging from semidiurnal to seasonal and interannual time scales. Provision of a realistic reproduction of the physical processes that regulate the water exchange between the Mediterranean Sea and the Atlantic Ocean at the Strait of Gibraltar is not straightforward. Recent works indicate that, in order to make realistic simulations of the water exchanges at Gibraltar, a model should have very high resolution [both in horizontal (about 500 m) and in vertical (about 10 m) directions], it should include explicit tidal forcing, and it should be implemented with physical parameterizations taking into account diapycnal mixing and entrainment (e.g., Sannino et al. 2009b, and references therein). A model that has these characteristics would be able to properly reproduce the small-scale mechanisms that govern the water flow through Gibraltar and its hydraulic criticality (Sannino et al. 2009a,b). However, the explicit representation of such small-scale processes in numerical models of the Mediterranean Sea designed for climate studies and therefore running over several decades is

extremely demanding on computing resources and, at the present, beyond the available resources at many research centers. Thus, also in the CIRCE models the Strait of Gibraltar is modeled using only few grid points and vertical levels and, in some cases, using relatively simple parameterizations for entrainment and mixing processes. Specifically, for the physical parameterization for entrainment and mixing processes applied at the strait, CMCC uses an upstream advection scheme for active tracers, while in the rest of the basin a monotonic upwind scheme for conservation laws (MUSCL; Van Leer 1979) is adopted. The vertical diffusivity in this area, between 30- and 150-m depths, is increased in order to parameterize unresolved processes induced by vertical mixing. In the same geographical area, the bottom friction drag coefficient is linear and 5 times larger than in the other parts of the model. ENEA increases the vertical diffusion 10 times with respect to the rest of the model in the strait area and replaces the horizontal bi-Laplacian viscosity with a Laplacian viscosity. MPI, CNRM, and LMD do not apply any specific parameterization (Dubois et al. 2012; Elizalde et al. 2010).

The simulations. The models described above have been used to make climate simulations of the second part of the twentieth century (1951–2000) and the first part of the twenty-first century (2001–50). During the twentieth-century period of the simulations, the distribution and concentration of the atmospheric greenhouse gases (GHGs) and aerosol (anthropogenic sulfate only) have been specified from observations, as it has been done for the CMIP3 twentieth-century integrations (20C3M; Meehl et al. 2007). During the twenty-first-century period, however, the GHGs and anthropogenic aerosol have been specified according to the IPCC Special Report on Emissions Scenarios (SRES) scenario A1B (Nakićenović and Swart 2000).

The model simulations have been initialized with the Levitus (Levitus 1982) or MedAtlas-II (MEDAR Group 2002) climatology as initial conditions for the ocean and either atmospheric reanalyses or the Atmospheric Model Intercomparison Project (AMIP) type of simulations (i.e., simulations where the atmospheric-only model has been integrated using observed SST as boundary conditions) for the atmosphere. A spinup of several decades of the coupled system has then been performed by integrating the model with the 1950s permanent conditions (radiative forcing). For example, in the case of the CMCC model, the global coupled system (global atmosphere and global ocean) has been integrated for about 200 yr and then the Mediterranean Sea model has been added to the system and another 50-yr spinup integration has been done. A similar spinup procedure has been used with the other models (for additional details, please see the references reported in Table 1) and in most of the cases it has allowed the models to reach a reasonably stable state (i.e., no significant long-term temperature drift was found for the upper ocean). Only in one case, the LMD model, is there some evidence that, despite the spinup, the bottom water of the Mediterranean Sea (deeper than 1,000 m) is still affected by a cooling trend at the beginning of the CIRCE integration that will affect the behavior of the whole water column for the earlier decades of the simulation, as we will see in the computation of the steric effect in the next section.

Once the model spinup has been completed, the GHGs and aerosols have been changed according to the 20C3M radiative forcing up to year 2000 and afterwards, from 2001 to 2050, following the A1B scenario. As shown in Table 1, the ENEA and MPI models have been integrated using boundary conditions from the 20C3M and A1B simulations performed with ECHAM5/MPI-OM (Giorgetta et al. 2006) and with the CMCC CIRCE simulation, respectively.

More detailed descriptions and in-depth discussions of the models' features and how the simulations have been conducted can be found in Dubois et al. (2012), Gualdi et al. (2012), and the documentation papers and reports listed in Table 1.

SOME RESULTS FROM THE CIRCE PROJECTIONS.
Here, we illustrate some basic findings obtained from the CIRCE simulations, with the aim of providing a quick overview and summary of the results of the CIRCE models and their potential, especially for climate change impact studies in the Mediterranean region. A more extended and detailed discussion of the results obtained from the CIRCE models can be found in Artale et al. (2010), Gualdi et al. (2012), Dubois et al. (2012), Elizalde (2011), and Dell'Aquila et al. (2011).

Overall, the CIRCE models appear to reproduce reasonably well many of the observed features related to the orographic forcing. Compared to the CMIP3 models, the simulation, for example, of the seasonal-mean precipitation over the northwest of the Iberian Peninsula, Alpine region, western coast of the Balkans, and southwest Anatolian Peninsula seems to be locally improved. Despite these local improvements, the overall model systematic errors over the region remain substantial, both in terms of 2-m land temperature (T2m) and precipitation

(Gualdi et al. 2012). During both winter [December–February (DJF)] and summer [June–August (JJA)], the models are generally colder than observations by about 2°C over most of the Mediterranean area.

Over land, larger errors, though confined to very small areas, are found locally in the northern foothills of the Alps (about −6°C), whereas a warm bias (about +4°C) covers the southeastern part of the Alpine region. The models tend also to overestimate the precipitation over central Europe in both seasons, whereas rainfall tends to be underestimated in the Alpine region; the Middle East; and, in JJA, the area of the Black Sea. A more detailed description of the CIRCE models' errors can be found in Gualdi et al. (2012).

Over the sea, the SST error appears to be rather uniform across the basin and can be explained by either too cold air–sea fluxes during the spinup integration coming from the atmospheric model or by the advection of too cold waters through the Gibraltar Strait (Dubois et al. 2012; Dell'Aquila et al. 2011).

Despite the systematic error, however, most of the CIRCE models reproduce reasonably realistic patterns of near-surface temperature and precipitation and a realistic structure of the Mediterranean SST, especially, of the observed SST gradients.

In order to provide an overall estimation of the capability of the CIRCE models in reproducing the main features of the observed Mediterranean climate, we computed the Taylor diagrams (Taylor 2001) of the T2m, precipitation, and SST seasonal means (Fig. 3). In this application, the simulated means are compared to the observed ones, with the spatial standard deviation and its associated root-mean-square difference (RMSD) plotted in relation to the pattern correlation. Specifically, Fig. 3 shows the Taylor diagrams of the simulated Mediterranean SST averaged over the basin and T2m and precipitation over land averaged over the Mediterranean area (28°–48°N, 9.5°W–38.5°E). The observations used in the analysis are T2m and precipitation obtained for the period 1971–2000 from the gridded observations [Climatic Research Unit Time Series (CRU TS) 3; Mitchell and Jones 2005] and the high-resolution SST reanalysis for the Mediterranean Sea (Adani et al. 2011) for the period 1985–2000. A similar analysis has been done using the Mediterranean SST from the Hadley Centre Global Sea Ice and Sea Surface Temperature dataset (HadISST; Rayner et al. 2003) for the period 1971–2000, and the results obtained are fully consistent with those shown in Figs. 3a,b.
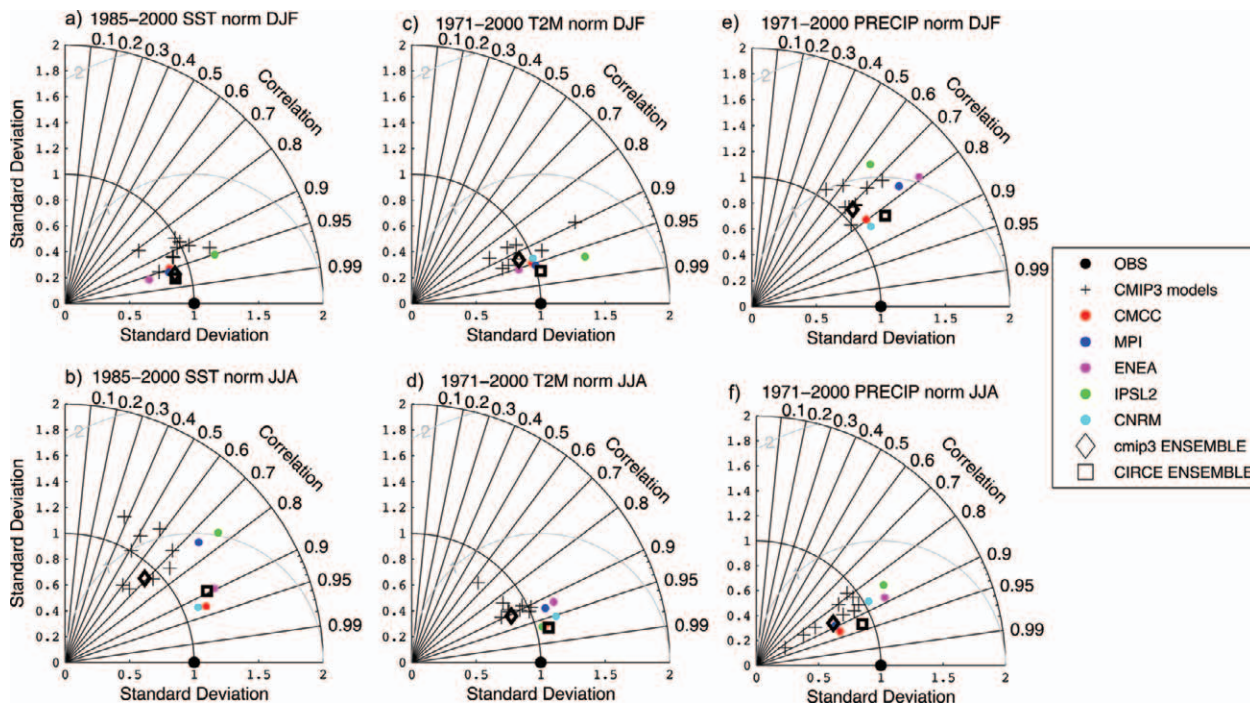
FIG. 3. Taylor diagrams of SST [(a) DJF and (b) JJA means], T2m over land [(c) DJF and (d) JJA means], and precipitation over land [(e) DJF and (f) JJA means]. The plot summarizes the pattern correlation, RMSD, and spatial standard deviation of each of the CMIP3 and CIRCE models with respect to observations [SST Mediterranean reanalysis (Adani et al. 2011) and CRU TS 3 (Mitchell and Jones 2005)] over the Mediterranean area (28°–48°N, 9.5°W–38.5°E).

Furthermore, to provide also a comparison between the CIRCE and the CMIP3 models' performance, we included in the diagrams the results obtained from a set of CMIP3 simulations. Importantly, the purpose of this work is neither to provide an exhaustive assessment of the differences between the CIRCE and the CMIP3 models nor to study all of the simulations available in the CMIP3 database. Thus, the set of CMIP3 models and simulations that we consider here is not comprehensive. With the 10 CMIP3 models presented in Table 2 and considered in the analysis, we expect to have a representative sample of the performance of state-of-the-art coupled models in simulating the Mediterranean region climate and its possible projected changes. More information about the CMIP3 models can be found on the CMIP3 website at the Program for Climate Model

Diagnosis and Intercomparison (PCMDI; http://www-pcmdi.llnl.gov/ipcc/model_documentation/ipcc_model_documentation.php).

Overall, the majority of CMIP3 models (indicated with a cross in the pictures of Fig. 3) underestimate the spatial standard deviation. In several cases, the CIRCE models (colored dots) appear to be closer to observations (black dot), though the spatial standard deviation of precipitation in DJF and T2m and SST in JJA tend to be slightly overestimated. Moreover, the majority of the CIRCE models have larger pattern correlations and smaller RMSDs than the CMIP3 ones. The Taylor diagrams of the multimodel ensemble means (indicated with a diamond for the CMIP3 case and with a square for the CIRCE case) give further evidence of the slight improvement of the CIRCE Mediterranean SST, land T2m, and land precipitation compared to the CMIP3 models.

TABLE 2. List of models and relative resolution (atmosphere and ocean). The grid interval is approximate, as it may vary across latitudes and may be different in the longitude and latitude directions. The reader is referred to the PCMDI website (http://www-pcmdi.llnl.gov) for more information on models and experiments.

Acronym	CMIP3 model name	Center	Atmospheric resolution	Oceanic resolution
BCCR	Bjerknes Centre for Climate Research Bergen Climate Model (BCCR-BCM2.0)	Bjerknes Centre for Climate Research (Norway)	$2.81° × 2.81°$ L31	$1.5° × (1.5° − 0.5°)$ L35
CNRM	CNRM CM3	Météo-France/CNRM (France)	$2.81° × 2.81°$ L45	$2° × (1.5° − 0.5°)$ L31
CSIRO	Commonwealth Scientific and Industrial Research Organisation Mark version 3.5 (CSIRO Mk3.5)	CSIRO Atmospheric Research (Australia)	$1.88° × 1.88°$ L18	$1.88° × 0.84°$ L31
GFDL	Geophysical Fluid Dynamics Laboratory Climate Model version 2.1 (GFDL CM2.1)	U.S. Department of Commerce/National Oceanic and Atmospheric Administration (NOAA)/GFDL (United States)	$2.5° × 2°$ L24	$1° × (1° − 0.33°)$ L50
IAP	Flexible Global Ocean–Atmosphere–Land System Model gridpoint version 1.0 (FGOALS-g1.0)	State Key Laboratory of Numerical Modeling for Atmospheric Sciences and Geophysical Fluid Dynamics (LASG)/Institute of Atmospheric Physics (IAP; China)	$2.81° × 2.81°$ L26	$1° × (1° − 0.33°)$ L30
IPSL	IPSL Coupled Model version 4 (CM4)	IPSL (France)	$3.75° × 2.5°$ L19	$2° × (1.5° − 0.5°)$ L31
MIROC	Model for Interdisciplinary Research on Climate 3.2, high-resolution version [MIROC3.2(hires)]	Center for Climate System Research/National Institute for Environmental Studies/Frontier Research Center for Global Change (CCSR/NIES/FRCGC) (Japan)	$1.1° × 1.1°$ L56	$0.28° × 0.19°$ L47
MPI	ECHAM5/MPI-OM	MPI (Germany)	$1.88° × 1.88°$ L31	$1.5° × 1.5°$ L40
NCAR	Community Climate System Model, version 3 (CCSM3)	National Center for Atmospheric Research (NCAR) (United States)	$1.4° × 1.4°$ L26	$1° × (1.1° − 0.27°)$ L40
UKMO	Third climate configuration of the Met Office Unified Model (HadCM3)	Hadley Centre for Climate Prediction and Research/Met Office (UKMO) (United Kingdom)	$3.75° × 2.5°$ L38	$1.25° × 1.25°$
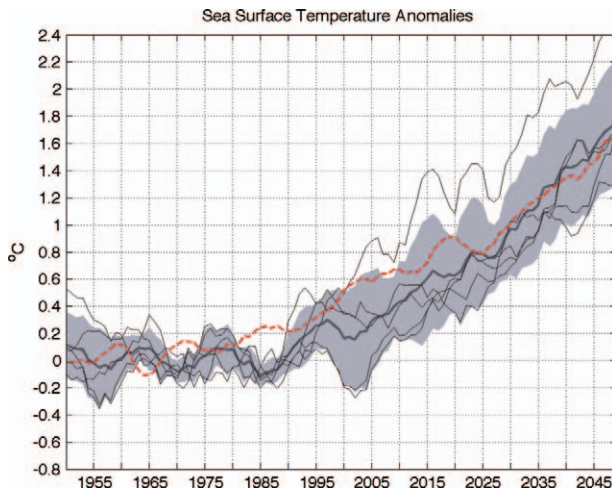
Fig. 4. Evolution of the SST anomalies from 1951 to 2050 as simulated with the CIRCE models (thin black lines) and with the CMIP3 models (red dashed line). The anomalies are expressed in °C and have been computed with respect to the 1961–90 mean. The thick black curve is the CIRCE multimodel mean, whereas the shading is the CIRCE multimodel standard deviation with respect to the multimodel mean. To highlight the long-term trends, the interannual variability has been filtered by applying 5-yr running mean.

Noteworthy, both in the CIRCE and CMIP3 ensembles, the multimodel means appear to be in better agreement with observations than any of the individual models. This result is consistent with previous findings (e.g., Glecker et al. 2008), where much wider ranges of physical variables were considered and analyzed. Pincus et al. (2008) suggested that the improvement associated with the multimodel means is generally due to both the spatial smoothing and the model systematic errors compensation performed by the multimodel averaging.

Finally, also the amplitude of the multiannual (interannual and decadal) variability (not shown) appears to be reasonably well captured by the CIRCE models in terms of both spatial distribution and amplitude, with maximum values of about 1°C.

Near-surface temperature and precipitation. The evolution of the simulated near-surface temperature averaged over the Mediterranean land during the recent past is in substantial agreement with the observations, showing that the region surrounding the Mediterranean Sea has been warming during most of the twentieth century. During the period 1951–2000 the ensemble-mean warming trend is about $0.1° \pm 0.04°C$ decade^{-1} (statistically significant at the 95% level, according to Mann–Kendall trend test). The increase of the low-level temperature is

found to have a remarkable spatial and seasonal modulation. During northern summer, the trend over western and central Europe appears to be larger than in the winter season. The largest trend (up to 0.2°C decade^{-1}) is found in JJA over the Iberian Peninsula and western part of North Africa. Importantly, the simulated trends found for the second half of the twentieth century are consistent with the results obtained from the observations for the instrumental period (1951–2005; Ulbrich et al. 2012).

A more in-depth discussion of the trends of T2m and precipitation observed in the Mediterranean region and a comparison between the observed values and the CIRCE simulations can be found in Ulbrich et al. (2012) and Gualdi et al. (2012).

The CIRCE projections for the twenty-first century suggest that remarkable changes in the climate of the Mediterranean region might occur already in the next few decades of the scenario, showing a rather steady increase of the near-surface temperature that leads the Mediterranean lands (i.e., the land within the area 28°–47°N, 10°W–40°E) to be substantially warmer at the end of the integration period with respect to the 1961–90 mean. The increment of the mean temperature is particularly pronounced in southern Europe and northern Africa in summer (JJA) and over the Alps, where during both the winter and summer seasons the projected 2021–50 mean warming appears to be as large as 2°C.

The evolution of the simulated Mediterranean SST (Fig. 4) shows no clearly discernible trends during the early period of the integration (1951–80); then a positive trend appears to emerge, starting from the second half of the 1980s. The mean SST warming found for the period 2021–50 compared to the reference period 1961–90 ranges between +0.8° and 1.8°C.

The regional characteristics of the projected changes in different subregions of the Mediterranean area are shown in Fig. 5, where the changes in mean T2m (right panels) and precipitation (left panels) are plotted. In particular, the pictures show the changes over seven subregions obtained as the differences between the mean for the period 2021–50 and the reference period 1961–90. The subregions are defined according to Giorgi and Lionello (2008) as follows: whole Mediterranean (Med), 28°–48°N, 9.5°W–38.5°E; northern Mediterranean (NMed), 41°–48°N, 9.5°W–38.5°E; southern Mediterranean (SMed), 28°–41°N, 9.5°W–38.5°E; western Mediterranean (WMed), 28°–44°N, 9.5°W–10.5°E; central Mediterranean (CMed), 28°–46°N, 10.5°–20.5°E; eastern Mediterranean (EMed), 28°–44°N, 20.5°W–38.5°E; and Alpine region (ALPS), 44°–48°N, 5.5°–15.5°E.

Figure 5 offers also the opportunity to compare the CIRCE-projected change with the signal obtained from the considered CMIP3 models. Furthermore, it provides a first assessment of the differences (spread) between the results obtained from the different CIRCE models (plus symbols), which are an important component of the uncertainties that affect the CIRCE projections.

The results shown in Fig. 5 (left) indicate that the projected warming appears to be relatively uniform across the considered subregions during JJA. In this season, all of the areas appear to be affected by a mean increase of T2m, which ranges between about 1.75° and 2°C in the CIRCE models and between 1.5° and 1.75°C in the CMIP3 ones. During winter (DJF; Fig. 5, top left), there are more pronounced differences

between the responses of the subregions to the radiative forcing. The Alpine region, for example, appears to be more sensitive, showing a larger warming, particularly pronounced in the CIRCE projections. Also, the spread of the results obtained from the different CIRCE models exhibits some substantial spatial and seasonal dependency. The difference between the model projections in the NMed and in the ALPS is significantly larger than the model spread found for the SMed or EMed, especially during northern winter. Importantly, during both seasons, there is a remarkable agreement between the CIRCE and CMIP3 T2m projected changes, at least in terms of their multimodel ensemble means.

The changes in precipitation (Fig. 5, right) show a clear tendency toward dryer conditions for the whole
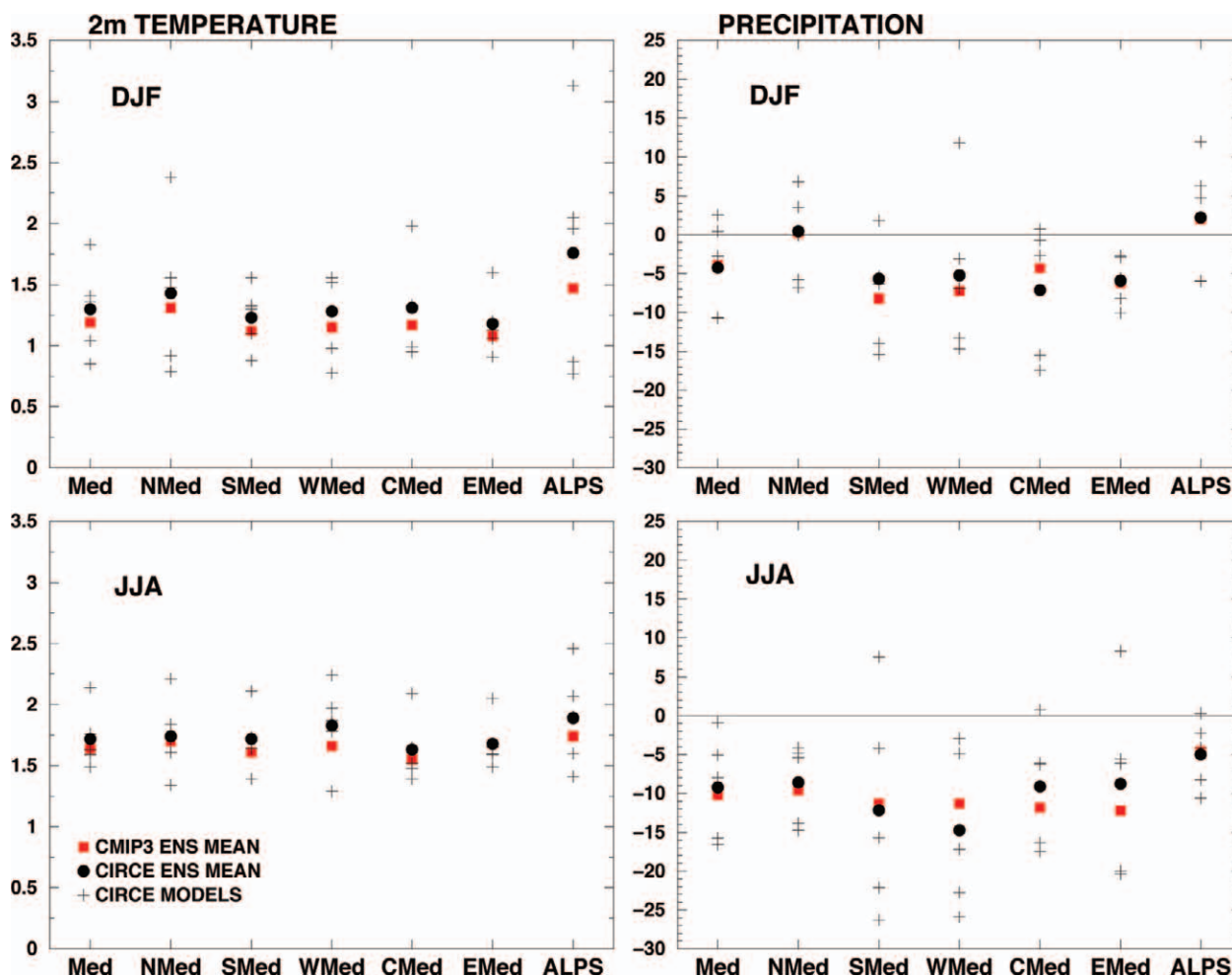

Fig. 5. Change in (left) seasonal-mean T2m and (right) mean precipitation obtained from the CIRCE and the CMIP3 simulations for the 2021–50 period compared to the reference (1961–90) period. The CIRCE models are indicated with the plus symbol, whereas the filled black circles represent the CIRCE multimodel ensemble means and the filled red squares represent the CMIP3 multimodel ensemble means. Shown are (top) the changes for the winter (DJF) and (bottom) the changes for the summer (JJA). The differences have been computed for seven areas of the Mediterranean region defined according to Giorgi and Lionello (2008). Units are °C for T2m and percentage of the reference period value for precipitation.

Mediterranean area, which is visible in both seasons but more pronounced during summer. Overall, the change in precipitation between the 2021–50 seasonal means and the seasonal means for the reference period is of about −5%. The model results show reduced rainfall over most of the subregions, even if the uncertainty due to the CIRCE model spread appears to be higher than for the T2m case. During summer (bottom-right panel), the reduction of precipitation appears to characterize all of the subregions, whereas in winter (top-left panel) the precipitation response appears to be different in the northern part of the Mediterranean area compared to the rest of the domain. Here, no substantial change (NMed) or even some rainfall increase (ALPS) is found, in agreement with the findings of Giorgi and Lionello (2008). Finally, also for the projected precipitation changes the results obtained from the CIRCE models appear to be remarkably consistent with the CMIP3 simulations, especially for the DJF season.

The tendency toward a warmer and dryer climate for the Mediterranean region in the next decades is consistent with the change in surface circulation suggested by the change found in the projected mean sea level pressure (MSLP; not shown). In DJF, a large area of increased MSLP covers the entire Mediterranean region, which, thus, appears to be characterized by increased anticyclonic circulation and enhanced stability. Furthermore, the increased anticyclonic circulation associated with the enhanced Mediterranean surface pressure is, in turn, associated with a northward shift of the Atlantic storm track. Both the increased stability and the northward displacement of the storm track have the effect of reducing the cyclonic activity in the Mediterranean basin, which is consistent with the decreased winter precipitation found in the projections. These results are in agreement with previous results based on the CMIP3 climate projections (Giorgi and Lionello 2008), with the trends in MSLP found in the observations during the instrumental period (Ulbrich et al. 2012) and with the PRUDENCE climate change projections (Christensen et al. 2007). The consensus that we see between the CIRCE projections and the results obtained from previous investigations leads us to think that these findings are considerably robust to substantial changes in the configuration of the climate models used to produce the scenario simulations.

Changes in the Mediterranean water budget. The trends in temperature and precipitation found in the CIRCE projections are also associated with a more vast change, involving the Mediterranean basin and its hydrologic cycle in particular. Over the land surrounding the Mediterranean basin, projected evaporation shows very little change in winter and a clear tendency to decrease in summer, whereas over the sea it appears to increase both in winter and in summer. Noteworthy, these findings are fully consistent with Held and Soden (2006). The projected value of the budget evaporation–precipitation (*E-P*) shows a marked positive trend, both over the sea and over the surrounding lands, due to the combined effect of increased evaporation and reduced precipitation, in agreement with results of Mariotti et al. (2008) and Sanchez-Gomez et al. (2009) obtained using the CMIP3 and the ENSEMBLES simulations, respectively.

The analysis of the simulated WB of the Mediterranean Sea and its various components (*E-P-R-B*, where *R* is the river runoff and *B* is the net freshwater flux coming from the Black Sea) shows that, in agreement with the observations, the Mediterranean Sea is an evaporative basin, with a net loss of water through the surface, compensated by a net water mass inflow from the Atlantic through the Strait of Gibraltar. Also, the values of the simulated water budget appear to be generally consistent with the observational data (~1.7 mm day^{-1}; Sanchez-Gomez et al. 2011). Figure 6 shows the evolution of the simulated WB of the Mediterranean basin for all of the CIRCE integrations. In the second half of the twentieth century, the simulated WB is characterized by some large variability but no clear long-term trends. In the second part of the integration period (2000–50), however, all of the models exhibit a WB significant positive trend, with an ensemble-mean value of approximately 0.07 ± 0.02 mm day^{-1} per decade. The WB increase for the projected period 2021–50 compared to the 1961–90 mean ranges between 0.15 (for the ENEA model) and 0.35 mm day^{-1} (for the CMCC model). In all of the simulations, these changes are mostly due to the decrease found in *P*, *R*, and *B* and the increase in *E*. Specifically, the model projections suggest that the increase in sea surface evaporation might be as large as +3% [close to the +2.9% found in Mariotti et al. (2008)], whereas the reduction in rainfall is of about −9% [larger than the −7.8% found in Mariotti et al. (2008)]. Therefore, according to the CIRCE projections, in the next decades the Mediterranean Sea might lose more water through its surface than in the recent past. Also in this case the CIRCE simulations appear to be in overall agreement with observations and the modeled tendencies are consistent in sign with those observed in the 1960–2000 period (Mariotti et al. 2008).

Changes in the Mediterranean heat budget. An analysis of the Mediterranean Sea surface heat budget (HB = SW + LW + LH + SH, where SW is the net surface shortwave radiation, LW is the net surface longwave radiation, LH is the latent heat flux, and SH is the sensible heat flux) shows that, for all of the CIRCE models, the net budget is negative at the Mediterranean Sea surface, meaning that there is a net heat loss from the sea surface. The simulated HB for the reference period ranges between −1.7 (ENEA model) and −6.4 W m^{-2} (LMD model), whereas the ensemble mean is −3.8 W m^{-2}. These values compare well with the observations [e.g., −7.0 W m^{-2} from Pettenuzzo et al. (2010) and −3.0 W m^{-2} from Sanchez-Gomez et al. (2011)], though individually the components of the model HB can differ from the observed ones. Noteworthy, the fact that all of the CIRCE models produce a negative heat budget in the Mediterranean basin and in reasonably good agreement with the observations is an important result. This feature, which is a well-known characteristic of the Mediterranean Sea, in fact, is generally not reproduced by atmospheric-only regional models (e.g., Sanchez-Gomez et al. 2011).

The simulated negative heat loss at the surface of the Mediterranean is compensated by a gain of heat from the Atlantic through the Strait of Gibraltar. During the control period, all of the CIRCE models show a net positive heat flux entering, through Gibraltar, into the Mediterranean Sea. The simulated values range between 2.3 and 6.3 W m^{-2}, well consistent with the estimates obtained from the observations (Sanchez-Gomez et al. 2011; Pettenuzzo et al. 2010).

The projected response for the next decades shows, in all of the models, an increase in SW heat gain (reduced cloud cover), a decrease in the LW heat loss (the increased incoming LW radiation due to the atmospheric greenhouse effect prevails on the increased outgoing LW radiation due to the higher SSTs), a decrease in the SH loss (the air–sea temperature gradient decreases as the atmosphere warms faster than the ocean), and an increase in the LH heat loss (increased evaporation). In all of the CIRCE simulations, the surface net heat loss decreases during the twenty-first-century projections and the projected response in the different heat flux components appears to be consistent among all models. The mean simulated HB for the period 2021–50 is of about −0.8 W m^{-2}, leading to a weaker cooling of the ocean by the atmosphere.

An extensive analysis of the Mediterranean water budget and heat budget as simulated by the CIRCE
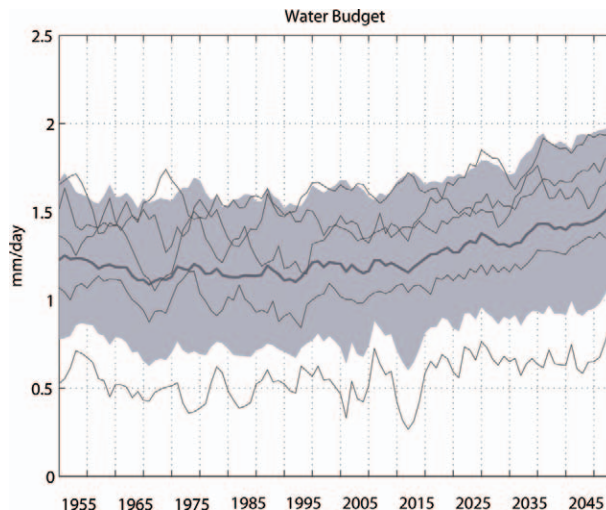
Fɪɢ. 6. As in Fig. 3, but for the water budget of the Mediterranean basin expressed in millimeters per day. The budget is computed as *E-P-R-B*.

models, including a detailed comparison with the observations and a discussion of the projected changes, is provided in Dubois et al. (2012).

Changes in the Mediterranean sea level. The CIRCE projections provide also an estimate of the possible sea level change in the Mediterranean Sea due to the steric effect, which for this basin has been shown to be quite substantial (Marcos and Tsimplis 2008). Combining tide-gauge observations and satellite products, Calafat et al. (2009) suggest that the steric effect in the Mediterranean Sea might produce a trend of sea level change of 0.3 cm yr^{-1} for the 1993–2000 period and 0.1 cm yr^{-1} for the 1961–2000 time interval. Figure 7 shows the evolution of the simulated steric sea level change in the CIRCE integrations from 1951 to 2050. During the reference period (1961–90), the ensemble-mean tendency is −0.07 ± 0.2 cm yr^{-1}. The models produce a rather broad range of trends, varying from the positive values of the ENEA and CNRM models (+0.16 and +0.17 cm yr^{-1}, respectively) to the relatively small negative values of the CMCC and MPI simulations (−0.16 and −0.13 cm yr^{-1}, respectively) to the large negative value found for the LMD case (−0.57 cm yr^{-1}). The large negative steric trend found in the reference period of the LMD simulation is most likely due to a remarkable negative temperature drift still present in the Mediterranean Sea water during the early decades of the integration. The cooling is particularly pronounced during the 1951–70 period (e.g., about −0.03°C yr^{-1} in the upper 1,000 m), and it is probably due to an incomplete spinup of the model.
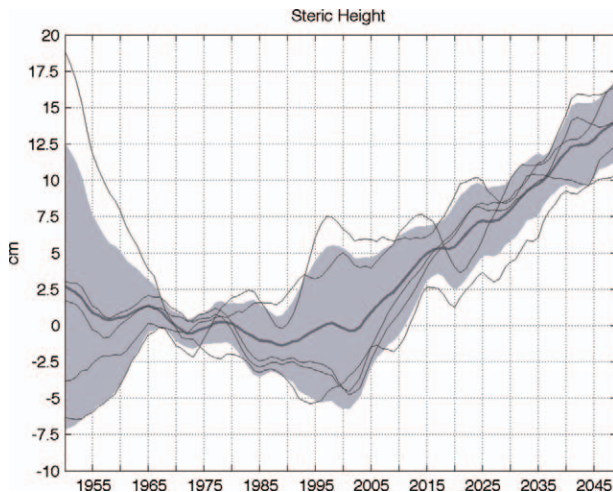
Fig. 7. As in Fig. 4, but for the steric component of the sea level change. The plotted values (cm) show the evolution of the simulated sea level change due to the steric effect. Steric anomalies are computed with respect to the reference period (1961–90).

Throughout the projected period, all of the CIRCE models show significant positive trends of the steric sea level change (0.29 ± 0.13 cm yr⁻¹). The 2021–50 mean steric sea level rise ranges between +7 and +12 cm, with respect to the reference period. Marcos and Tsimplis (2008), using the A1B CMIP3 simulations, found that the steric effect for the Mediterranean Sea at the end of the twenty-first century might account for an average sea level change ranging between −22 and +18 cm. In the CIRCE projections, therefore, the range of sea level change appears to be significantly reduced compared to the results of Marcos and Tsimplis (2008). However, the relatively small number of models that form the CIRCE ensemble does not allow for performing a robust uncertainty assessment. Therefore, with the present results, we cannot attribute the smaller spread to an actual reduction of the uncertainty produced, in turn, by the improved representation of the Mediterranean Sea in the models.

Finally, it is noteworthy that the CIRCE range of steric change is consistent also with Tsimplis et al. (2008), where at the end of a twenty-first-century SRES A2 projection performed with a coupled atmosphere–ocean regional climate model (Somot et al. 2008) the basin-averaged sea level rise is of about 13 cm.

CONCLUDING REMARKS. The CIRCE project has made substantial efforts to improve the simulations of the climate of the Mediterranean region, with the aim of providing more reliable climate change projections for this area. In particular, we enhanced the representation of the Mediterranean Sea in the climate system by including ocean components permitting mesoscale circulation features in the Mediterranean basin. For the first time, the evolution of some key sea variable (e.g., SST, SSS, sea level, and water and heat fluxes) can be obtained at high resolution over the Mediterranean Sea and with a high degree of physical consistency due to coherent air–sea flux modeling by dedicated coupled atmosphere–ocean models.

When compared with the CMIP3 simulations, the CIRCE models show some improvement in reproducing the seasonal means of T2m, precipitation, and SST. However, the CIRCE simulations, which include high-resolution air–sea coupling in the Mediterranean region, show significant systematic errors in near-surface temperature and precipitation. Such errors are locally larger than those obtained with regional high-resolution atmospheric-only models (e.g., the ENSEMBLES models).

The CIRCE models provide a reasonably good estimate of the Mediterranean water budget and especially of the surface heat budget. In contrast with most of the ENSEMBLES models, the total heat budget in all of the CIRCE simulations is negative for the present period, with values in good agreement with observations, satisfying the heat closure budget controlled by the heat transport through Gibraltar, also consistent with the observational results.

The CIRCE projections indicate that remarkable changes in the Mediterranean region climate might occur already in the early few decades of the scenario. A substantial warming (almost 1.5°C in winter and almost 2°C in summer) and a significant decrease of precipitation (about 5%) might affect the region in the 2021–50 period compared to the reference period (1961–1990), in an A1B emission scenario. However, locally the changes might be even larger. The projected surface net heat loss decreases in the projected period, leading to a weaker cooling of the Mediterranean Sea by the atmosphere. In contrast, the water budget appears to increase in the next decades, leading the Mediterranean Sea to lose more water through its surface than in the past. Furthermore, according to the CIRCE projections, the climate change might induce a 2021–50 mean steric sea level rise that ranges between +7 and +12 cm, with respect to the period of reference.

The climate change projections obtained from the CIRCE models are overall consistent with the findings obtained in previous scenario simulations, such as PRUDENCE, ENSEMBLES, and CMIP3. The agreement leads to thinking that these findings are

robust to substantial changes in the configuration of the climate models used to produce the scenario simulations. The consensus between the CIRCE projections and the previous findings, especially those obtained from PRUDENCE and ENSEMBLES, shows also that, in general terms, the regional air–sea coupling does not impact strongly the response to anthropogenic climate change.

The CIRCE results show also a nonnegligible spread, which is most likely due to differences in the models physics and in the experimental setup, such as the use of global and limited-area model configurations, with the latter integrated with boundary conditions coming from different global simulations. Also, it is likely that the introduction of the air–sea coupling in the CIRCE simulations contributes to the spread of the responses, although a size of five ensemble members does not allow testing it in a statistical sense. An increase in spread, however, does not necessarily imply an increase in uncertainty in the CIRCE simulations with respect to the results obtained with uncoupled models. The use of uncoupled regional models, as, for example, in ENSEMBLES or PRUDENCE, introduces an underestimated uncertainty because the models neglect the physical processes associated with the two-way interaction between atmosphere and ocean, which might be important, as shown in Somot et al. (2008) and Artale et al. (2010).

Finally, it is important to keep in mind that, despite some improvements, the CIRCE models still have large systematic errors. Therefore, to increase the reliability of the climate change projections, further efforts are required to reduce the biases introduced by the regional air–sea coupling.

The most evident and pronounced systematic error in the CIRCE simulations is the cold bias that appears to affect the entire region. As has been discussed in Dubois et al. (2012), this bias might arise from different sources such as too cold Atlantic water entering at Gibraltar and atmospheric air temperature boundary conditions. However, also problems in the model physical parameterizations (e.g., the surface albedo, especially over the Mediterranean Sea) might contribute to the error.

The models discussed here can be improved in many ways, by either trying to reduce the systematic errors or improving the representation of important processes. As a first step, for example, the parameterization of the surface albedo over the Mediterranean Sea could be improved by introducing a dependency on the zenith angle. The change in the albedo representation might have an impact of more than 15 W m^{-2} on the net shortwave radiation (Dubois et al. 2012), thus affecting the surface temperature. Also the representation of the fresh water input, both from the river discharge and the Black Sea, should be enhanced, improving further the water balance of the basin. Moreover, in order to provide more accurate estimates of the possible Mediterranean Sea level rise, the local and remote effects of the atmospheric pressure should be included in the ocean model equations.

The regional climate simulations performed within CIRCE represent the first attempt to address the possible climate change in the Mediterranean area using a set of coupled numerical models able to represent the basic physical properties of the Mediterranean Sea, with a multimodel approach. They have represented a seminal effort that will be continued and improved in new international programs and initiatives such as the Hydrological Cycle in the Mediterranean Experiment (HyMeX; Drobinski and Ducrocq 2008) and the Mediterranean Coordinated Regional Climate Downscaling Experiment (Med-CORDEX; Ruti et al. 2011).

REFERENCES

Adani, M., S. Dobricic, and N. Pinardi, 2011: Quality assessment of a 1985–2007 Mediterranean Sea reanalysis. *J. Atmos. Oceanic Technol.,* **28,** 569–589.

Artale, V., and Coauthors, 2010: An atmosphere-ocean regional climate model for the Mediterranean area: Assessment of a present-climate simulation. *Climate Dyn.,* **35,** 721–740.

Beuvier, J., and Coauthors, 2010: Modeling the Mediterranean Sea interannual variability over the last 40 years: Focus on the EMT. *J. Geophys. Res.,* **115,** C08017, doi:10.1029/2009JC005950.

Calafat, F. M., D. Gomis, and M. Marcos, 2009: Comparison of Mediterranean sea level fields for the period 1961–2000 as given by a data reconstruction and a 3D model. *Global Planet. Change,* **68,** 175–184.

Christensen, J. H., T. R. Carter, M. Rummukainen, and G. Amanatidis, 2007: Evaluating the performance and utility of regional climate models: The PRUDENCE project. *Climatic Change,* **81,** 1–6.

——, M. Rummukainen, and G. Lenderink, 2009: Formulation of very-high-resolution regional climate model ensembles for Europe. ENSEMBLES: Climate change and its impacts at seasonal, decadal and centennial timescales, P. van der Linden and J. F. B. Mitchell, Eds., Met Office Hadley Centre Rep., 47–58.

Dell'Aquila, A., S. Calmanti, P. M. Ruti, M. V. Struglia, G. Pisacane, A. Carillo, and G. Sannino, 2011: Impacts of seasonal cycle fluctuations over the Euro-Mediterranean area using a regional ocean-atmosphere coupled model. *Climate Res.,* **52,** 135–157, doi:10.3354/cr01037.

Déqué, M., and Coauthors, 2007: An intercomparison of regional climate simulations for Europe: Assessing uncertainties in model projections. *Climatic Change,* **81** (Suppl.), 53–70.

Drobinski P., and V. Ducrocq, 2008: HYdrological cycle in the Mediterranean EXperiment: Towards a major field experiment in 2010–2020. White Book. [Available online at www.hymex.org/public /documents/WB_1.3.2.pdf.]

Dubois, C., and Coauthors, 2012: Future projections of the surface heat and water budgets of the Mediterranean Sea in an ensemble of coupled atmosphere–ocean regional climate models. *Climate Dyn.,* **39,** 1859–1884, doi:10.1007/s00382-011-1261-4.

Elizalde, A., 2011: The water cycle in the Mediterranean region and the impacts of climate change. Max Planck Institute for Meteorology Rep. on Earth System Science 103, 128 pp.

——, D. Sein, U. Mikolajewick, and D. Jacob, 2010: Technical report: Atmosphere-ocean-hydrology coupled regional climate model. Max Planck Institute for Meteorology Tech. Rep., 5 pp. [Available online at www.remo-rcm.de/fileadmin/user_upload/remo /UBA/pdf/TechnicalReport.pdf.]

Gao, X. J., J. S. Pal, and F. Giorgi, 2006: Projected changes in mean and extreme precipitation over the Mediterranean region from a high resolution double nested RCM simulation. *Geophys. Res. Lett.,* **33,** L03706, doi:10.1029/2005GL024954.

Gibelin, A. L., and M. Déqué, 2003: Anthropogenic climate change over the Mediterranean region simulated by a global variable resolution model. *Climate Dyn.,* **20,** 327–339.

Giorgetta, M. A., G. P. Brasseur, E. Roeckner, and J. Marotzke, 2006: Preface to special section on climate models at the Max Planck Institute for Meteorology. *J. Climate,* **19,** 3769–3770.

Giorgi, F., 2006: Climate change hot-spots. *Geophys. Res. Lett.,* **33,** L08707, doi:10.1029/2006GL025734.

——, and P. Lionello, 2008: Climate change projections for the Mediterranean region. *Global Planet. Change,* **63,** 90–104.

Glecker, P. J., K. E. Taylor, and C. Doutriaux, 2008: Performance metrics for climate models. *J. Geophys. Res.,* **113,** D06104, doi:10.1029/2007JD008972.

Gualdi, S., and Coauthors, 2012: Future climate projections. *Regional Assessment of the Climate Change in the Mediterranean: Air, Sea and Precipitation and Water,* A. Navarra and L. Tubiana, Eds., Advances in Global Change Research, Vol. 50, Springer Verlag, 125.

Hagemann, S., and D. Jacob, 2007: Gradient in the climate change signal of European discharge predicted by a multi-model ensemble. *Climatic Change,* **81** (Suppl.), 309–327.

Held, I. M., and B. J. Soden, 2006: Robust responses of the hydrological cycle to global warming. *J. Climate,* **19,** 5686–5699.

Hourdin, F., and Coauthors, 2006: The LMDZ4 general circulation model: Climate performance and sensitivity to parametrized physics with emphasis on tropical convection. *Climate Dyn.,* **27,** 787–813.

Levitus, S., 1982: *Climatological Atlas of the World Ocean.* NOAA Prof. Paper 13, 173 pp. and 17 microfiche.

López-Moreno, J. I., M. Beniston, and J. M. García-Ruiz, 2008: Environmental change and water management in the Pyrenees: Facts and future perspectives for Mediterranean mountains. *Global Planet. Change,* **61,** 300–312.

Ludwig, W., E. Dumont, M. Meybeck, and S. Heussner, 2009: River discharges of water and nutrients to the Mediterranean Sea: Major drivers for ecosystem changes during past and future decades? *Prog. Oceanogr.,* **80,** 199–217.

Marcos, M., and M. N. Tsimplis, 2008: Comparison of results of AOGCMs in the Mediterranean Sea during the 21st century. *J. Geophys. Res.,* **113,** C12028, doi:10.1029/2008JC004820.

Mariotti, A., and Coauthors, 2008: Mediterranean water cycle changes: Transition to drier 21st century conditions in observations and CMIP3 simulations. *Environ. Res. Lett.,* **3,** 044001, doi:10.1088/1748-9326/3/4/044001.

MEDAR Group, 2002: *MEDATLAS 2002 Database: Cruise Inventory, Observed and Analyzed Data of Temperature and Bio-Chemical Parameters.* IFREMER, 4 CD-ROMs.

Meehl, G. A., C. Covey, T. Delworth, M. Latif, B. McAvaney, J. F. B. Mitchell, R. J. Stouffer, and K. A. Taylor, 2007: The WCRP CMIP3 multimodel dataset—A new era in climate change research. *Bull. Amer. Meteor. Soc.,* **88,** 1383–1394.

Mitchell, T. D., and P. D. Jones, 2005: An improved method of constructing a database of monthly climate observations and associated high-resolution grids. *Int. J. Climatol.,* **25,** 693–712.

Nakićenović, N., and R. Swart, Eds., 2000: *Special Report on Emissions Scenarios.* Cambridge University Press, 599 pp.

Oddo, P., M. Adani, N. Pinardi, C. Fratianni, M. Tonani, and D. Pettenuzzo, 2009: A nested Atlantic-Mediterranean Sea general circulation model for operational forecasting. *Ocean Sci.,* **5,** 461–473.

Oki, T., and Y. C. Sud, 1998: Design of Total Runoff Integrating Pathways (TRIP)—A global river channel network. *Earth Interact.,* **2.** [Available online at http://EarthInteractions.org.]

Pettenuzzo D., W. Large and N. Pinardi, 2010: On the corrections of ERA-40 surface flux products consistent with the Mediterranean heat and water budgets and the connection between basin surface total heat flux and NAO. *J. Geophys. Res.,* **115,** C06022, doi:10.1029/2009JC005631.

Pincus, R., C. P. Batstone, R. J. P. Hofmann, K. E. Taylor, and P. J. Glecker, 2008: Evaluating the present-day simulation of clouds, precipitation, and radiation in climate models. *J. Geophys. Res.,* **113**, D14209, doi:10.1029/2007JD009334.

Rayner, N. A., D. E. Parker, E. B. Horton, C. K. Folland, L. V. Alexander, D. P. Rowell, E. C. Kent, and A. Kaplan, 2003: Global analyses of sea surface temperature, sea ice, and night marine air temperature since the late nineteenth century. *J. Geophys. Res.,* **108,** 4407, doi:10.1029/2002JD002670.

Ruti, P., and Coauthors, 2011: MED-CORDEX initiative for Mediterranean climate studies. *Geophysical Research Abstracts,* Vol. 13, Abstract EGU2011-10715. [Available online at http://meetingorganizer.copernicus.org/EGU2011/EGU2011-10715.pdf.]

Sanchez-Gomez, E., S. Somot, and A. Mariotti, 2009: Future changes in the Mediterranean water budget projected by an ensemble of regional climate models. *Geophys. Res. Lett.,* **36,** L21401, doi:10.1029/2009GL040120.

——, ——, S. A. Josey, C. Dubois, N. Elguindi, and M. Déqué, 2011: Evaluation of the Mediterranean Sea water and heat budgets as simulated by an ensemble of high resolution regional climate models. *Climate Dyn.,* **37,** 2067–2086, doi:10.1007/s00382-011-1012-6.

Sannino, G., M. Herrmann, A. Carillo, V. Rupolo, V. Ruggiero, V. Artale, and P. Heimbach, 2009a: An eddy-permitting model of the Mediterranean Sea with a two-way grid refinement at the Strait of Gibraltar. *Ocean Modell.,* **30,** 56–72, doi:10.1016/j.ocemod.2009.06.002.

——, L. Pratt, and A. Carillo, 2009b: Hydraulic criticality of the exchange flow through the Strait of Gibraltar. *J. Phys. Oceanogr.,* **39,** 2779–2799.

Scoccimarro, E., and Coauthors, 2011: Effects of tropical cyclones on ocean heat transport in a high-resolution coupled general circulation model. *J. Climate,* **24,** 4368–4384.

Somot, S., F. Sevault, and M. Déqué, 2006: Transient climate change scenario simulation of the Mediterranean Sea for the 21st century using a high-resolution ocean circulation model. *Climate Dyn.,* **27,** 851–879.

——, ——, ——, and M. Crépon, 2008: 21st century climate change scenario for the Mediterranean using a coupled atmosphere-ocean regional climate model. *Global Planet. Change,* **63,** 112–126.

Taylor, K. E., 2001: Summarizing multiple aspects of model performance in a single diagram. *J. Geophys. Res.,* **106** (D7), 7183–7192.

Thorpe, R., and G. Bigg, 2000: Modelling the sensitivity of the mediterranean outflow to anthropogenically forced climate change. *Climate Dyn.,* **16,** 355–368.

Tsimplis, M., M. Marcos, and S. Somot, 2008: 21st century Mediterranean sea level rise: Steric and atmospheric pressure contributions from a regional model. *Global Planet. Change,* **63,** 105–111, doi:10.1016/j.gloplacha.2007.09.006.

Ulbrich, U., and Coauthors, 2012: Past and current climate changes in the Mediterranean region. *Regional Assessment of the Climate Change in the Mediterranean: Air, Sea and Precipitation and Water,* A. Navarra and L. Tubiana, Eds., Advances in Global Change Research, Vol. 50, Springer Verlag, 125.

Valcke, S., 2006: OASIS3 user guide (prism_2–5). CERFACS Tech. Rep. TR/CMGC/06/73, PRISM Rep. 3, 60 pp.

Van Leer, B., 1979: Towards the ultimate conservative difference scheme. V. A second-order sequel to Godunov's method. *J. Comput. Phys.,* **32,** 101–136.

Zou, L., Z. Tianjun, L. Li, and Z. Jie, 2010: East China summer rainfall variability of 1958–2000: Dynamical downscaling with a variable-resolution AGCM. *J. Climate,* **23,** 6394–6408.